KOREAN JOURNAL OF PACKAGING SCIENCE & TECHNOLOGY
Vol. 21, No. 3 107~113 (2015)
http://dx.doi.org/10.20909/kopast.2015.21.3.107

A Study of Thermal Properties of LDPE-Nanoclay Composite Films

Nattinee Bumbudsanpharoke and Seonghyuk Ko*

Department of Packaging, Yonsei University, 1 Yonseidaegil, Wonju-si, Gangwon-do, 220-710 Korea

Abstract This work focused on the study of thermal properties and kinetic behavior of LDPE-nanoclay composite films. The effect of nanoclay content (0.5, 1, 3, and 5 wt%) on thermal stability and crystallization characteristics of the nanocomposites were investigated by Thermogravimetric Analysis (TGA) and Differential Scanning Calorimetry (DSC). The results from endothermic curve showed that the nanoclay played an important role in the crystallization of nanocomposites by acting as nucleating agent. From exothermic curve, there was a crystallization temperature shift which was attributed to crystallization process induced by nanoclay. The TGA results showed that the addition of nanoclay significantly increased the thermal stability of LDPE matrix, which was likely due to the characteristic of layered silicates/clays dispersed in LDPE matrix as well as the formation of multilayered carbonaceous-silicate char. A well-known Coats-Redfern method was used to evaluate the decomposition activation energy of nanocomposite. It was demonstrated that introducing of nanoclay to LDPE matrix escalated the activation energy of nanocomposite decomposition resulting in thermal stability improvement.

Keywords LDPE-nanoclay composite, Thermal properties, Coats-Redfern model

Introduction

Low density polyethylene (LDPE) is a semicrystalline thermoplastic polymer which is widely used in food packaging, medical care, insulator and other industrial sectors[1,2]. Conventional microfillers are incorporated to LDPE for further improvement of its thermal and mechanical performances, but additions of large volume content (20-30 wt%) are required to achieve the desired properties[3]. The large content of microfillers generally interfere the system and leads to poor processability. On the contrary, only very small amounts of nanofiller (generally lower than 5 wt%)[4] are needed to bring up some large improvements to the polymer matrix. Recently, polyethylene-clay nanocomposites have attracted considerable attention[5].

Organic montmorillonite (OMMT) or layered silicates is widely used in a range of applications due to their availability and low cost[4]. It makes ordinary polymer become an advanced material with increasing strength and heat resistance, decreasing gas permeability and flammability, and improving biodegradability of biodegradable polymer[6,7]. To acquire the desired properties, nanoclay should be evenly dispersed and distributed in the polymer matrix. Generally, the clay is not easy to be dispersed into low polarity polymer such as polyolefin because they preferred arranging themselves as face-to-face stacking in agglomerated tactoid pattern[8].

The inorganic particles with nanoscale dimension can lead to ultra-large interfacial area between the constituents. The very large polymer/layered-inorganic interface alters the molecular mobility, the relaxation behavior, and the consequent thermal and mechanical properties of the resulting nanocomposite material[4]. The aim of this study is to investigate the effects of organoclay on the thermal properties of the low density polyethylene nanocomposites (LDPE-nanoclay). The kinetic parameters of thermal decomposition of the nanocomposites were extensively studied via a well-known Coats-Redfern method.

†Corresponding Author : Seonghyuk Ko
Department of Packaging, Yonsei University, Wonju 220-710, Korea
Tel: +82-33-760-2299, Fax: +82-33-760-2299
E-mail : s.ko@yonsei.ac.kr

Material and Methods

Materials

LDPE (Lutene LB7500, LG Chemical Co., Yeosu, Korea) was used in the study. It has had a melt flow index (MFI) of 7.5 g/10 min (ASTM D1238) and a density of 0.918 g/cm^3. The nanoMax®-LDPE is used as masterbatch and it contains 50 wt% of Nanomer® nanoclay (I.44P, Nanocor Inc. Hoffman Estates, USA).

Preparation of LDPE-nanoclay composite films

The LDPE-nanoclay composite films were prepared by melt-extruding to yield composite films with nanoclay loading

contents of 0, 0.5, 1, 3, and 5 wt%. The composite films were processed with a laboratory-scale, twin-screw extruder (BA-19, BauTek Co., Uijeongbu, Korea) with a length/diameter (L/D) ratio of 40:19. LDPE and nanoclay masterbatch pellets were dried in a convection oven at 80°C for 24 h prior to extrusion and mixed in a sealed plastic bag by manual tumbling before being fed into the extruder. The respective temperatures for the eight different processing zones from the feeder to horizontal header of the extruder were set as 110/110/180/190/185/180/175/170°C and the screw speed rate was maintained at 300 rpm. The composite films were maintained at a thickness of approximately 60 μm to facilitate the evaluation of physical properties.

Fourier-transform infrared (FTIR)

Fourier-transform infrared (FTIR) spectra were recorded with a Perkin Elmer Spectrum 65 spectrophotometer in attenuated total reflection (ATR) mode with C/ZnSe crystal; sixteen scans with resolution 2 cm^{-1} in the wave number range of 400-4000 cm^{-1} were performed. For each sample 5 spectra were performed on the exposure surface and spectra were collected in transmittance mode.

Field-emission scanning electron microscope (FE-SEM)

The surface morphology and cross section of the composite sheet were observed with a field-emission scanning electron microscope (FE-SEM Quanta FEG 250, FEI, USA) after sputtering platinum/palladium onto the specimen using a Cressington Sputter Coater 108 auto (Cressington Scientific Instruments, Watford, UK). Further elemental analysis was carried out with an energy-dispersive X-ray spectrometer (EDS, Ametek, USA) attached to the FE-SEM.

Thermogravimetric analysis (TGA)

Thermogravimetric analysis (TGA) was performed on TGA 4000 thermogravimetric analyzer (PerkinElmer Co. Ltd., Massachusetts, USA). The sample was heated from 30°C to 800°C at a rate of 10°C·min^{-1} under a nitrogen flow rate of 20 mL·min^{-1}.

Differential scanning calorimetry (DSC)

Non-isothermal crystallization study was taken on a DSC Q20 instrument (TA Instruments, Castle, USA). About 5-6 mg of samples was accurately weighted and encapsulated in a typical aluminium pan. An empty sealed pan was used as a reference. All the DSC tests were conducted under nitrogen atmosphere. The samples were heated with a constant rate of 10°C·min^{-1} from 30°C to 250°C (1st heating scan) and held for 5 min to erase their thermal or morphological history and to permit complete melting of the previous crystals. Subsequently, samples were cooled down to 60°C at a constant rate of 10°C·min^{-1} (cooling scan) to study the crystallization behavior. Finally, the samples were heated again for the second time (2nd heating scan) at 10°C·min^{-1} to 250°C to melt the crystals that have been formed during the cooling scan and to find the melting temperature of each sample. All DSC curves were normalized to the unit weight of the sample.

Results and Discussion

Chemical interaction between LDPE and nanoclay

FTIR is a technique widely used to characterize the presence of specific chemical groups in the materials. Fig. 1 illustrates the infrared spectra of LDPE and LDPE-nanoclay composites with different clay contents. The assignment of FTIR spectra of nanoclay is listed in Table 1. An obvious absorption peak at about 464, 521, and 1,047 cm^{-1} can be found for the nanoclay composite sample; this is a typical IR absorption peak of silica (Si) and aluminium (Al), originating from stretching and bending mode[9]. The characteristic of nanoclay spectra became stronger with the higher nanoclay content in composite system.

Morphology

The cross-section morphology of the LDPE-nanoclay composite film was observed using FE-SEM and EDS analyses were carried out after being imaged. In Fig. 2, the cross-sec-

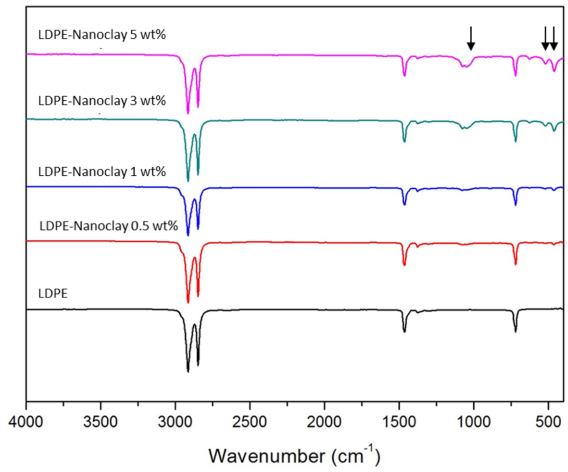

Fig. 1. FTIR spectra of LDPE and LDPE-nanoclay composites.

Table 1. Assignment of FTIR spectra of nanoclay

Wavenumber (cm^{-1})	Major Functional Group
464	Si-O bending
521	Al-O stretching
1,047	Si-O stretching

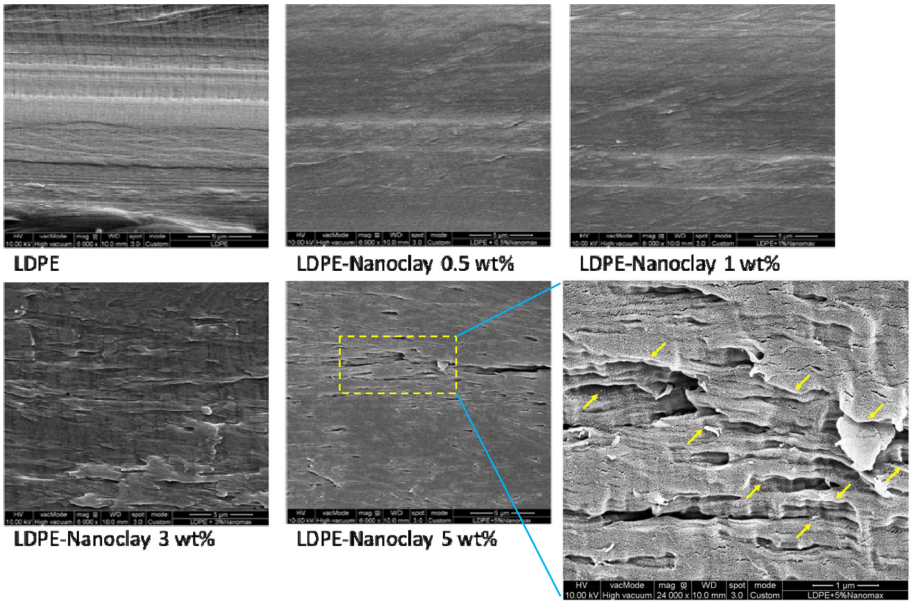

Fig. 2. SEM micrographs of cross section of neat LDPE and LDPE-nanoclay composites at 6,000X magnification.

tion surface of the neat LDPE presents a continuous phase without any voids, whereas the surface with higher nanoclay displays a micro-void structure. This segregated surface could be from the dispersion of nanoclay in LDPE system. As seen in Fig. 2, there is no layered clay morphology found on composite with below 3 wt% clay content. On the other hand, tactoid and intercalated structure appear oriented practically parallel to the film surfaces at the higher clay content (i.e., 3 and 5 wt% clay content). At 5 wt% clay content nanocomposite, the SEM micrograph illustrates the predominant multilayers structure inside LDPE matrix (pointed out with yellow arrows) which could be from the dispersion of clay platelets. Table 2 shows the presence of Al and Si from coordinated EDS result. The concentration of these elements increases toward the concentration of nanoclay loading.

Thermal stability

The thermal degradation of a polymer is usually determined by a thermogravimetric analysis (TGA) in terms of weight percent in the sample as a function of temperature. The important parameters are the onset temperature of the degradation ($T_{10\%}$), which is measured as the point in which 10% of the sample is lost, and the mid-point of the degradation ($T_{50\%}$)[6]. Table 3 and Fig. 3 present the TGA weight loss (%) profiles against temperature. Thermal stability of the nanocomposite is enhanced comparing to that of neat LDPE. At $T_{10\%}$, the results showed that initial thermal degradation of the nanocomposites are all much higher than that of neat LDPE (437°C). The $T_{10\%}$ value of the nanocomposites increases with increasing nanoclay loading and the maximum value was 464°C at 5 wt% nanoclay content. The similar result was reported in other literatures[6,10]. The improvement in the thermal stability can be explained through the formation of insulating and incombustible multilayered carbonaceous–silicate char forming on composite surface during combustion. This char will obstruct the escape or diffusion of low molecular weight volatile products within the nanocomposites, and also insulate the underlying polymer from surrounded heat[6,11,12]. Additionally, the physical-chemical adsorption of the volatile decomposition products on the silicates/clays could delay the volatilization of the products that are generated from carbon-carbon bond scission in the LDPE matrix[8]. As expected, the residue at 600°C of all the nanocomposites samples corresponds rather well to the inorganic clay loading in the system. This is because nanoclay is inorganic materials which are incombustible in the temperature ranges that LDPE are decomposed into volatile compounds[13].

The Coast-Redfern equation is quite useful approach to evaluate the kinetic parameters for thermal degradation of the nanocomposites[8,14]. Considering the first order reaction and

Table 2. EDS analysis of nanoclay components in composite films

EDS-Cross Section	Al %wt	Si %wt
LDPE	0.00	0.00
LDPE-Nanoclay 0.5 wt%	0.62	0.22
LDPE-Nanoclay 1 wt%	0.73	0.22
LDPE-Nanoclay 3 wt%	0.75	0.28
LDPE-Nanoclay 5 wt%	0.92	1.07

Table 3. TGA data of LDPE-nanoclay composites in nitrogen

Sample	Temperature at 10% weight loss (°C)	Temperature at 50% weight loss (°C)	Residue (%)	E_d (kJ·mol^{-1})	R^2
LDPE	437	476	2.80	214.12	0.999
LDPE-Nanoclay 0.5 wt%	450	484	0.71	307.14	0.995
LDPE-Nanoclay 1 wt%	450	486	1.97	327.70	0.993
LDPE-Nanoclay 3 wt%	461	491	2.57	419.99	0.994
LDPE-Nanoclay 5 wt%	464	493	4.08	424.70	0.993

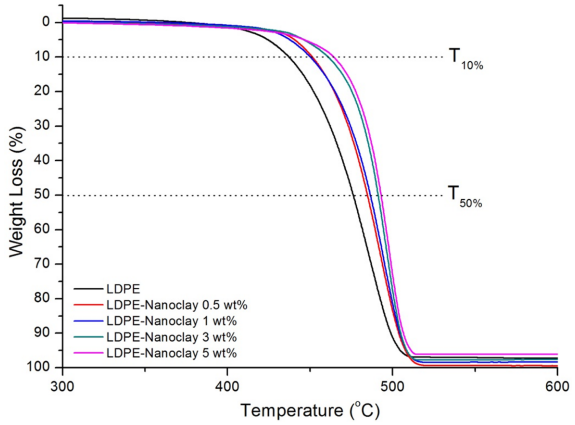

Fig. 3. TGA profiles of LDPE-nanoclay composite films.

random nucleation mechanism, the Coast-Redfern equation can be written as follows:

$$\ln\left(\frac{-\ln(1-\alpha)}{T^2}\right) = -\frac{E_d}{RT} + \ln\frac{AR}{\beta E_d} \quad (1)$$

where E_d is the activation energy (in this case, it is the decomposition activation energy), A is the pre-exponential factor, R is the universal gas constant (8.314 J mol^{-1} K^{-1}), β is the heating rate (10°C·min^{-1}), and T is the degradation temperature (K). The α represents the degree of conversion which is determined with weight loss at given temperature (T). In TGA analysis, α represents the kinetic conversion of a polymer into volatile decomposition products and it is defined as follows:

$$\alpha = \frac{m_i - m_T}{m_i - m_f} \quad (2)$$

where m_i is the initial sample weight, m_T is the weight of sample at temperature T, and m_f is the final sample weight. Plotting $\ln(-\ln(1-\alpha)/T^2)$ against $1/T$ (K) based on Eq. (1) will give a linear trend-line whose slope $(-\varepsilon_d/R)$ is directly proportional to the decomposition activation energy of the nanocomposites.

In this study, the kinetic parameters of thermal decomposition were investigated at the major decomposition temperature. The temperature range is 470-510°C with weight loss ranging 40-80%. Fig. 4 illustrates the Coats-Redfern plots for the nanocomposite decomposition step. The regression coefficient (R^2) and estimated E_d values corresponding to the thermal decomposition of the neat LDPE and LDPE-nanoclay composite films for the selected temperature range are listed in Table 3. R^2 values of all samples were close to unity (> 0.990) indicating the linear regression model is appropriate. The decomposition activation energy (E_d) of the nanocomposites is higher than that of neat LDPE, and increases with increasing nanoclay content. The higher value of E_d for the nanocomposite films infers that higher energy than that of neat LDPE is required to remove the volatile decomposition product. This kinetic analysis result suggests that an improved thermal stability of the nanocomposites is associated with the increase in the decomposition activation energy.

Thermal analysis

Thermal properties, such as melting temperature, crystallization temperature, fusion enthalpy, and crystallinity of non-isothermal crystalline of LDPE-nanoclay composites were studied with DSC analysis. The degree of crystallinity was calculated as expressed by the following equation:

$$X_c = \frac{\Delta H_m}{\Delta H_m^0} \times 100 \quad (3)$$

where ΔH_m represents the experimental heat of fusion (Jg^{-1}), ΔH_m^0 represents the theoretical heat of fusion of 100% crystalline LDPE (293Jg^{-1})[15]. The melting temperatures (T_m) as well as heat of fusion during the second heating are shown in Table 4. Crystallization temperature (T_c) was defined as the maximum temperature of the transition exothermic curve, whereas the crystallization onset temperature (T_{oc}) was taken as the temperature where the cooling curve initially departs from the curve baseline.

Fig. 5 is DSC curves of LDPE-nanocaly composite films. As seen in Fig. 5(a) and Table 4, the melting temperature (T_m) was slightly moved toward lower temperature as nanoclay content increases. This could be from the effect of difference in crystal properties (crystal type, packing density, crystallite size, and distribution etc.) between nanocomposite and neat

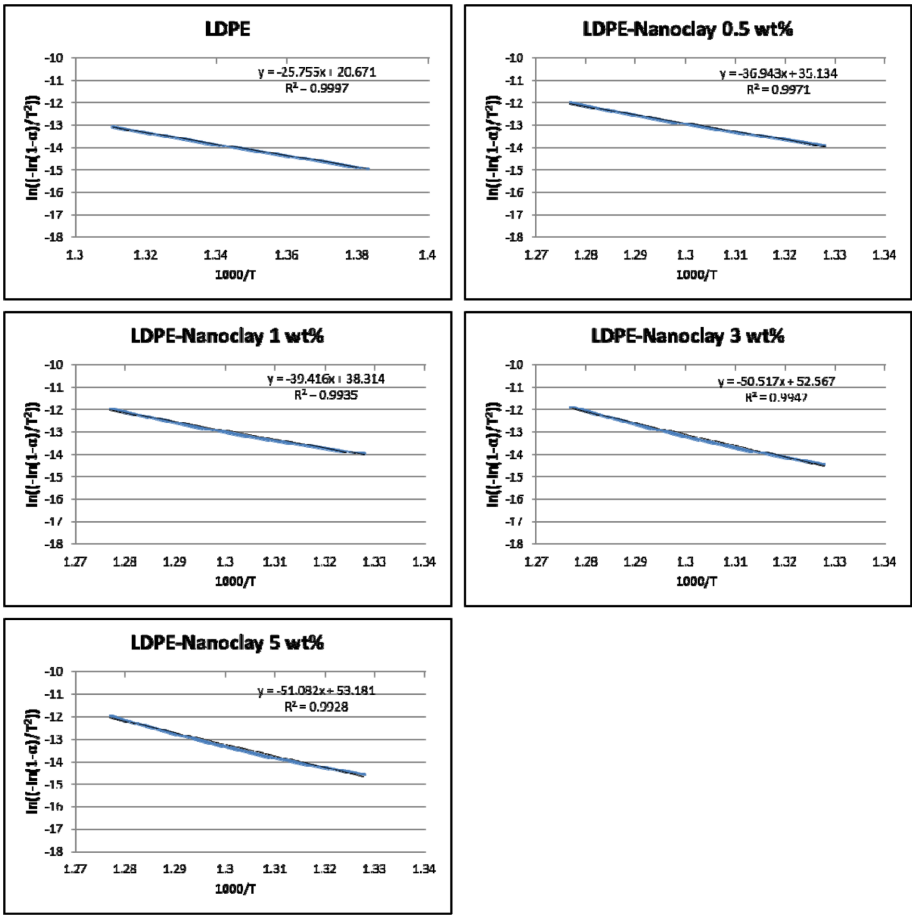

Fig. 4. Coats-Redfern plot of neat LDPE and LDPE-nanoclay composites.

Table 4. Melting temperatures, melting enthalpy, crystallinity, and crystalline temperature determined by DSC analysis

Sample	*T*m (°C)	Melting Enthalpy ($J \cdot g^{-1}$)	Crystallinity (%)	*T*c (°C)	*T*oc (°C)
LDPE	107.01	161.0	54.95	91.57	94.15
LDPE-Nanoclay 0.5 wt%	105.87	170.0	58.02	91.63	94.64
LDPE-Nanoclay 1 wt%	105.98	179.0	61.09	92.00	95.57
LDPE-Nanoclay 3 wt%	106.42	180.5	61.60	93.01	96.41
LDPE-Nanoclay 5 wt%	106.11	162.0	55.29	93.23	96.92

LDPE[4-6]. Study from Monica A, et al.[16] revealed that nanoclay layers acted as nucleating agents and facilitated the crystal growth by providing a higher level of nucleation density[6]. This may involve a crystal formation and attribute to the change of T_m. Moreover, increasing clay contents to 3 wt% significantly escalated the melting enthalpies and crystallinity of LDPE. Result shows that an increase of 12% crystallinity for the nanocomposite was obtained which could be suggested that there is nucleation effect of the filler in LDPE matrix[6]. Monica A, et al.[16] reported that the crystallinity of LDPE/PE-g-MA/OMMT increased with increase of OMMT and the maximum of crystallinity was found at 3% OMMT. However, they found that the crystalline level was dropped with further increase of OMMT content. From our result, the degree of crystallinity was found to decrease with further increases of nanoclay concentration at 5 wt%. A possible reason for this behavior was due to the "suppression effect" of clay at high content suggested by Homminga, et al.[17] and Mudaliar, et al.[18]. The explanation of such behavior is that the levels of perfection of the crystals are affected by the restricted mobility

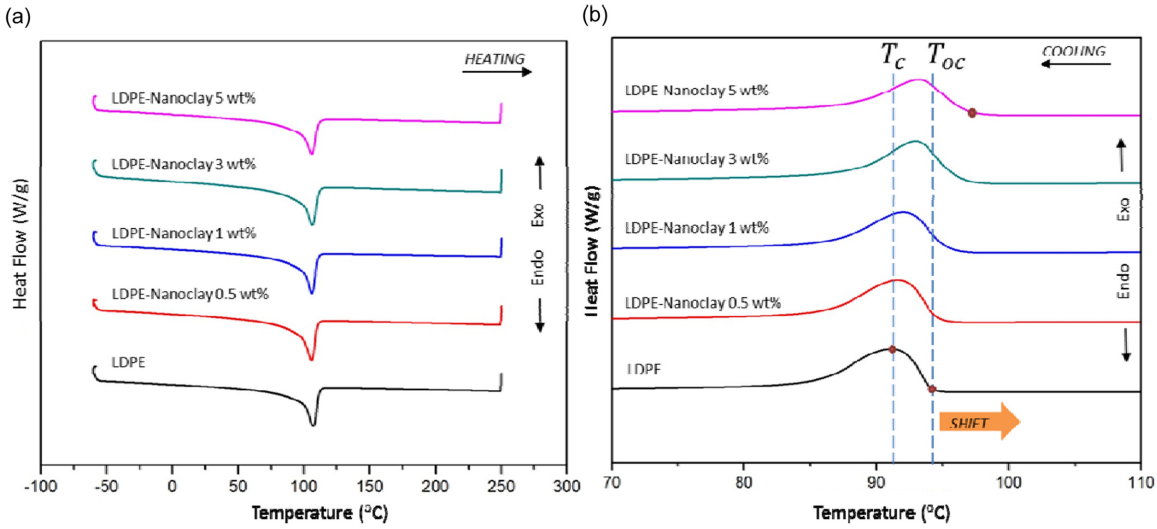

Fig. 5. DSC non-isothermal melting (a) and cooling (b) curves of LDPE-nanoclay composites.

of the LDPE chain segments, which retards the growth of well-developed lamellar crystals. This restriction increases with increasing nanoclay content resulting in less perfect crystals. An excessive amount of nucleation sites and retarded crystal growth lead to production of fine crystal and consequently result in a lower degree of crystallinity[18-22].

Fig. 5(b) shows the DSC non-isothermal cooling curves of the nanocomposites. As seen in the figure, the crystallization curves of the LDPE-nanoclay composites have been shifted in the y-direction to make them distinguishable. There is also a noticeable difference in the onset crystallization temperature (T_{oc}). The T_{oc} of the nanocomposites is about 2.77°C higher than that of neat LDPE, implying that nanoclay affects the nucleation forming temperature of polymer crystal[23]. It is likely because the nucleating effect of the nanoclay leads to the creation of nuclei on the crystallization process of the nanocomposites[8,16] where it starts at higher temperatures than the neat LDPE.

Conclusion

In this study, a series of clay nanoparticles loaded LDPE nanocomposites films were prepared by laboratory-scale twin-screw extruder. The FESEM micrographs showed the layered structure, which is attributed to the dispersed nanoclay in the LDPE matrix. Crystallinity of nanocomposite films was increased due to the nucleation effect of nanoclay. Beyond 3 wt% clay content, however, the crystallinity was dropped due to the suppression effect and less perfect crystals. The crystallite formation in LDPE was slightly accelerated and T_c was moved to slightly higher temperatures. Incombustible inorganic substances from nanoclay provided a multilayered carbonaceous-silicate acting as an effective surface shield to retard the thermal decomposition of volatile components and to prevent the transport of decomposed volatile products in the polymer composites. Coast-Redfern method demonstrates that the improving in thermal stability of the nanocomposites is influenced by the increase in the decomposition activation energy.

Acknowledgements

This research was supported by a grant (15162MFDS031) from Ministry of Food and Drug Safety in 2015.

References

1. Murray, K. A., Kennedy, J. E., McEvoy, B., Vrain, O., Ryan, D., and Higginbotham, C. L. 2012. The effects of high energy electron beam irradiation on the thermal and structural properties of low density polyethylene. Radiation Physics and Chemistry 81: 962-966.
2. Guastavino, F., Torello, E., Squarcia, S., Tiemblo, P., and Garcia, N. 2014. Insulation properties of LDPE nanocomposites obtained by the dispersion of different nanoparticles. Ieee Transactions on Dielectrics and Electrical Insulation 21: 444-451.
3. Balakrishnan, H., Hassan, A., Wahit, M. U., Yussuf, A. A., and Razak, S. B. A. 2010. Novel toughened polylactic acid nanocomposite: Mechanical, thermal and morphological properties. Materials & Design 31: 3289-3298.
4. Sorrentino, A., Gorrasi, G. and Vittoria, V. 2007. Potential perspectives of bio-nanocomposites for food packaging applications. Trends in Food Science & Technology 18: 84-95.
5. Qi, R. R., Jin, X. and Zhou, C. X. 2006. Preparation and properties of polyethylene-clay nanocomposites by an in situ

graft method. Journal of Applied Polymer Science 102: 4921-4927.
6. Olewnik, E., Garman, K. and Czerwinski, W. 2010. Thermal properties of new composites based on nanoclay, polyethylene and polypropylene. Journal of Thermal Analysis and Calorimetry 101: 323-329.
7. Ray, S. S. and Okamoto, M. 2003. Polymer/layered silicate nanocomposites: a review from preparation to processing. Progress in Polymer Science 28: 1539-1641.
8. Chafidz, A., Kaavessina, M., Al-Zahrani, S. and Al-Otaibi, M. N. 2014. Polypropylene/organoclay nanocomposites prepared using a Laboratory Mixing Extruder (LME): crystallization, thermal stability and dynamic mechanical properties. Journal of Polymer Research 21: 1-18.
9. Zazoum, B., David, E. and Ngô, A. 2013. LDPE/HDPE/clay nanocomposites: effects of compatibilizer on the structure and dielectric response. Journal of Nanotechnology 2013:
10. Silva, B. L., Nack, F. C., Lepienski, C. M., Coelho, L. A. F. and Becker, D. 2014. Influence of intercalation methods in properties of clay and carbon nanotube and high density polyethylene nanocomposites. Materials Research 17: 1628-1636.
11. Hemati, F. and Garmabi, H. 2011. Compatibilised LDPE/LLDPE/nanoclay nanocomposites: I. Structural, mechanical, and thermal properties. The Canadian Journal of Chemical Engineering 89: 187-196.
12. Modesti, M., Lorenzetti, A., Bon, D. and Besco, S. 2006. Thermal behaviour of compatibilised polypropylene nanocomposite: Effect of processing conditions. Polymer Degradation and Stability 91: 672-680.
13. Zhang, J. G., Jiang, D. D. and Wilkie, C. A. 2006. Thermal and flame properties of polyethylene and polypropylene nanocomposites based on an oligomerically-modified clay. Polymer Degradation and Stability 91: 298-304.
14. Kar, E., Bose, N., Das, S., Mukherjee, N. and Mukherjee, S. 2015. Enhancement of electroactive β phase crystallization and dielectric constant of PVDF by incorporating GeO_2 and SiO_2 nanoparticles. Physical Chemistry Chemical Physics 17: 22784-22798.
15. Wunderlich, B. and Czornyj, G. 1977. A study of equilibrium melting of polyethylene. Macromolecules 10: 906-913.
16. Monica A, P., Bernabé L, R., Karla A, G.-M., Víctor H, C.-R., Miguel, M., Johanna, C. and Álvaro, M. 2014. Low density polyethylene (LDPE) nanocomposites with passive and active barrier properties. Journal of the Chilean Chemical Society 59: 2442-2446.
17. Homminga, D. S., Goderis, B., Mathot, V. B. F. and Groeninckx, G. 2006. Crystallization behavior of polymer/montmorillonite nanocomposites. Part III. Polyamide-6/montmorillonite nanocomposites, influence of matrix molecular weight, and of montmorillonite type and concentration. Polymer 47: 1630-1639.
18. Mudaliar, A., Yuan, Q. and Misra, R. 2006. On surface deformation of melt-intercalated polyethylene-clay nanocomposites during scratching. Polymer Engineering & Science 46: 1625-1634.
19. Zazoum, B., David, E. and Ngô, A. D. 2014. Structural and dielectric studies of LLDPE/O-MMT nanocomposites. Transactions on electrical and electronic materials 15: 235-240.
20. Chen, J. B., Xu, J. Z., Xu, H., Li, Z. M., Zhong, G. J. and Lei, J. 2015. The crystallization behavior of biodegradable poly(butylene succinate) in the presence of organically modified clay with a wide range of loadings. Chinese Journal of Polymer Science 33: 576-586.
21. Di Maio, E., Iannace, S., Sorrentino, L. and Nicolais, L. 2004. Isothermal crystallization in PCL/clay nanocomposites investigated with thermal and rheometric methods. Polymer 45: 8893-8900.
22. Kontou, E. and Niaounakis, M. 2006. Thermo-mechanical properties of LLDPE/SiO_2 nanocomposites. Polymer 47: 1267-1280.
23. Grigoriadi, K., Giannakas, A., Ladavos, A. and Barkoula, N. M. 2013. Thermomechanical behavior of polymer/layered silicate clay nanocomposites based on unmodified low density polyethylene. Polymer Engineering and Science 53: 301-308.

투고: 2015.11.16 / 심사완료: 2015.12.26 / 게재확정: 2015.12.23